STBC-based hybrid precoding with DFT codebook construction in Massive MIMO Systems

Homeyra Rahbari [1*], Behzad Mozaffari Tazekand[1]

[1]*Electrical Engineering Faculty, University of Tabriz, Tabriz, Iran*

ABSTRACT

Millimeter wave (mmWave) communication, which utilizes massive multiple input multiple output (MIMO) techniques, is one of the key enabling technologies for high capacity 5G cellular networks. However, the hardware complexity and the high power consumption in massive-MIMO array hinder its integration. Hybrid precoding technique, which combines large-dimensional analog preprocessing with low-dimensional digital processing can be used to reduce both hardware costs and power consumption in massive MIMO systems, as a potential method. In this paper, we introduce a hybrid precoding structure design in both narrowband and wideband massive MIMO inspired by the effective alternating minimization (AltMin) algorithm with the Least Squares Amendment (LSA). To be specific, in the proposed design, the analog Radio Frequency (RF) precoder structure employs the Discrete Fourier Transform (DFT) processing which in turn affects the performance of the system. In addition, the proposed design relies on Space-Time Block Coding (STBC) to attain diversity and further enhances the system reliability. We evaluate bit error rate (BER) performance of proposed massive MIMO system using various hybrid precoding techniques. Numerical simulations (Monte Carlo) are performed to check the precision of proposed BER analytical expression. Our simulation results demonstrate significant performance gains of the proposed STBC-based hybrid precoding with DFT processing over existing hybrid precoding algorithms.

1. INTRODUCTION

1.1. Background

Millimeter wave (mmWave) multiple input multiple output (MIMO) systems, utilizing hybrid analog and digital precoding, represent one of the most promising techniques for future communication networks. In mmWave MIMO systems, the use of small wavelengths allows for the placement of many antennas in a compact space. However, employing large antenna arrays increases the number of Radio Frequency (RF) chains, leading to higher costs and power consumption [1]. The hybrid precoding scheme leverages the limited scattering property inherent in mmWave systems to minimize the number of required RF chains [2].

Hybrid Massive MIMO employs a two-step processing scheme (baseband and RF) which is illustrated in Fig. 1. This approach requires fewer RF chains compared to fully digital processing structures. The hybrid analog-digital architecture (that utilize switches, phase shifters, and RF lenses) offers wireless system designers a flexible mechanism to effectively balance performance with hardware complexity [3].

1.2. Related Works

Reference [4] has focused on the development of a multi-user massive MIMO hybrid beamforming system by comparing the effects of changing variables, such as the number of antennas and the type of modulation, to achieve higher data rates that approach those of a fully digital system with low complexity. They have designed

* Corresponding author
E-mail address: h_rahbari@tabrizu.ac.ir
https://orcid.org/0000-0003-0107-2543

analog and digital beamformers separately at the transmitter and receiver to maximize the total sum rate by utilizing the Minimum Mean Square Error (MMSE) technique. In addition, to enhance the performance of a fully digital massive MIMO structure, they jointly designed RF and baseband filters using orthogonal matching pursuit (OMP). Reference [5] proposes an alternating algorithm that applies a penalty method based on a partially-connected structure. The work indicates that the proposed system exhibits low computational complexity while delivering significant performance gains. Research findings on narrowband massive MIMO suggest that the performance of the hybrid structure is close to the optimal performance of a fully digital structure [6]. The design problem of hybrid precoders can be framed as minimizing the Euclidean distance between the unconstrained optimal solution and the hybrid precoders. In [6], three alternating optimization algorithms based on different principles are proposed to design the hybrid precoding matrix, with the goal of finding a precoding vector that minimizes this Euclidean distance. The factorization problem is divided into two unrelated optimization subproblems: non-convex quadratically constrained quadratic programming (QCQP) and unit-modulus least squares (ULS). Although their proposed algorithms outperform previously suggested methods, they also exhibit very high complexity.
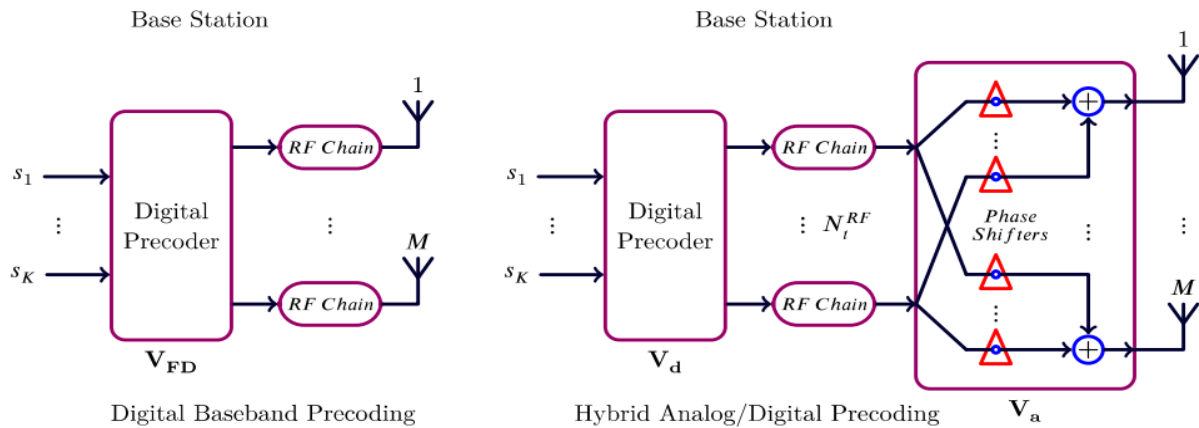
Fig. 1. Massive MIMO Architecture

The use of phase shifting networks in analog precoders has become challenging due to hardware implementation complexity and high power consumption. Typically, a single-phase shifter is used to connect an RF chain to an antenna, which imposes limitations on unit modulus. To overcome this algorithmic problem, [7] proposed a new scheme for designing hybrid precoders in multi-user OFDM mmWave MIMO systems by adopting a dual phase shifter (DPS). Their algorithms are developed for two structures (fully-connected and partially-connected).

The authors in [8] proposed a dynamic hybrid precoding structure that utilizes a switch network to provide flexible connections between phase shifters and antennas. The proposed method aims to enhance spectral efficiency while reducing power consumption compared to traditional fully-connected architectures. The study demonstrates that this dynamic approach can significantly improve energy efficiency and overall system performance in millimeter-wave communication scenarios.

To generate orthogonal beams with low power losses and cost, the Butler matrix based on Discrete Fourier Transform (DFT) processing was introduced in [9]. The Butler networks for implementing the DFT in RF analog precoding provide better performance than fully-connected structure in the hybrid precoding design [10]. Results in [11] confirm that the performance of hybrid precoding based on DFT is comparable to that of hybrid precoding architectures utilizing quantized phase shifters. The authors in [12] enhanced the equivalent channel gain by extending the dimensions of the analog precoding matrix into a square matrix and representing the codebook with a DFT matrix. They also employed an improved block diagonal scheme for digital precoding to reduce complexity and inter-user interference.

A two-step Alternating Minimization (AltMin) algorithm, utilizing a codebook for single-user narrowband scenarios, is proposed in [13]. This approach reduces complexity and outperforms previous algorithms. In the first step, a low-complexity codebook-based algorithm is employed. Instead of initializing the RF analog precoder with random phases, orthogonal-based matching pursuit (OBMP) is used to select the analog precoder columns from a DFT codebook. The second step employs the AltMin algorithm to refine the hybrid precoders. Most existing research on hybrid massive MIMO has focused on narrowband massive MIMO systems [13][14].

Limited attention has been paid to wideband hybrid precoding systems. The approach proposed in [15] formulates the problem of designing hybrid precoding for Orthogonal Frequency Division Multiplexing (OFDM) systems. This scheme dynamically divides users into several groups. The DFT-based user clustering hybrid precoding algorithm implemented at the base station consists of two parts: a DFT beamforming layer that creates orthogonality among user groups, and a linear multiuser MIMO precoding layer that facilitates spatial multiplexing within these

groups. Their algorithm is applicable to both fully-connected and partially-connected structures.

A related body of work has considered the spatial diversity process, where the same information is transmitted across all available multipath propagation paths to improve the reliability of the communication link. The first Space-Time Block Code (STBC) scheme, introduced by Alamouti, is capable of providing diversity gain [16]. Space-time codes enhance both the data rate and reliability of transmission but may struggle to adapt to the increasing density of multiuser massive MIMO systems. By utilizing STBC, data is organized in the form of a matrix, where the number of columns corresponds to the number of transmitter antennas and the number of rows corresponds to the time slots allocated for data transmission.

The main challenge in multi-user scenarios is that different signals experience distinct unknown space-time block coding (STBC) signals, propagation delays, and channel coefficients. Additionally, the STBC identification process is disrupted by multiple access interference. An evaluation of an experimental wireless communication technique called space-time coded massive (STCM) MIMO is presented in [17]. The STCM-MIMO system utilizes two massive transmit antenna arrays to transfer data to a single-antenna user. In [18], the authors introduced a novel multi-user scheme with an STBC-MIMO configuration that employs OFDM as a transmission framework. The bit error rate (BER), throughput error rate (TER), and peak-to-average power ratio (PAPR) performances of their scheme, based on computer simulations, demonstrate significantly higher performance compared to conventional systems.

The analyzes simulations of Orthogonal Space-Time Block Codes (OSTBC) are discussed in [19]. The results demonstrate how STBC improve data rates and can effectively reduce bit error rates (BER) by leveraging spatial diversity.

While most literature focuses on the energy consumption and complexity of hybrid precoding, further improvements are still needed in both the performance of hybrid precoding algorithms and their complexity.

1.3. Contributions

In this paper, we investigate the hybrid precoding in multiuser mmWave system with ability to provide high throughput. Millimetre wave communication is an effective approach to satisfy the capacity requirements of wireless communication systems and 5G networks. Our detailed contributions are summarized as follows:

- This study employs the Alternating Minimization (AltMin) algorithm, integrated with the Least Squares Amendment (LSA), as the primary design principle for hybrid precoding. Effective AltMin algorithms conceptualize the design of hybrid precoders as a matrix factorization problem. Furthermore, the digital precoding matrix is enhanced through LSA following the iterative results obtained from the algorithm. The algorithm

accepts an optimal unconstrained precoder as input and approximates it as a linear combination of beam steering vectors, which can subsequently be applied to the RF chain.

- We present a design for multiuser hybrid massive MIMO systems utilizing a DFT codebook-based analog precoder. Instead of random phase initialization, the columns of the analog precoder are selected from an orthogonal DFT codebook. The complexity of the codebook-based algorithm, which derives the precoder from a fixed set of orthogonal codewords, is generally much lower than that of non-codebook-based algorithms. This approach results in significantly lower complexity compared to non-codebook-based algorithms, making the hybrid precoding scheme with DFT processing an efficient low-complexity application.

- Due to the high bandwidth characteristic of mmWave systems, it is essential to consider hybrid precoding design when employing multi-carrier techniques such as OFDM, particularly to mitigate multi-path fading. In this work, we extend the proposed algorithm to the OFDM-based massive MIMO framework for wideband scenarios. Practically, by adopting OFDM, we can transform wideband frequency-selective fading channels into multiple parallel narrowband frequency-flat fading channels.

- We present a novel processing architecture that leverages the advantages of the Space-Time Block Coding (STBC) scheme in hybrid massive MIMO systems. A critical issue that requires further investigation in conventional massive MIMO systems is their reliability under severe fading conditions in wireless communication. By transmitting multiple versions of a data stream using the STBC scheme, the base station (BS) can obtain channel state information (CSI) for each user in real-time, thereby enhancing the reliability of data transmission [20]. This approach significantly improves the range and reliability of transmitted signals without necessitating increased bandwidth.

- In this paper, we analyze the performance of the bit error rate (BER) in the proposed massive MIMO system by providing an approximate BER formula for q-QAM modulation. Additionally, we present Monte Carlo simulations to evaluate the analytical BER expression. The numerical results confirm the validity of our closed-form analysis. We offer extensive comparisons to provide valuable design insights related to the proposed schemes. Our simulation results demonstrate that the performance of the proposed space-time block coding (STBC) hybrid massive MIMO technology approaches that of fully digital systems and outperforms conventional hybrid architectures.

Consequently, the proposed design proves to be beneficial for practical massive MIMO implementations.

1.4. Organization

We organize the rest of this paper as follows: In section 2, the mmWave MIMO system model in both narrowband and wideband channels is described and the optimization model is formulated. Section 3 shows new hybrid analog and digital precoder design massive MIMO. In this section, a novel algorithm is presented, subsequently the developed wideband hybrid precoding design will be analysed. In addition, the complexity analysis is presented in section 4 and the proposed hybrid precoding design are evaluated in section 5. Finally, section 6 are considered to the conclusions.

1.5. Notations

The lower-case and upper-case bold letters are used for vectors and matrices, respectively. The operations $[.]^*$, $[.]^T$ and $[.]^\dagger$ signify the complex conjugate, the transpose and the Hermitian transpose. $\mathbf{I}_N$ is the $N \times N$ identity matrix. $\| . \|$ denotes the Euclidean norm.

2. SYSTEM DESCRIPTION

Both narrowband and wideband transmission models of hybrid precoding massive MIMO system are described in the following.

2.1. System Model: Narrowband Transmission

In the following, we describe a system model for the downlink hybrid precoding system. We assume that the BS is equipped with M antennas to transmit data to K users and there are N_t^{RF} RF chains at the transmitter. The channel coefficients between users and BS are independent and identically distributed (i.i.d.) Rayleigh fading. The channel vector of kth user is denoted as $\tilde{\mathbf{h}}_k \in \mathbb{C}^{M \times 1}, k = 1,\ldots,K$ whose entries are i.i.d. $\mathcal{CN}(0,\delta_k)$ where δ_k represents large scale fading. To model favourable propagation, these channel vectors should be pair-wisely orthogonal. The downlink channel from BS to all users is defined as $\mathbf{H} = [\tilde{\mathbf{h}}_1, \tilde{\mathbf{h}}_2,\ldots,\tilde{\mathbf{h}}_K]$.

In the hybrid precoding structure, $\mathbf{V}_a = [\mathbf{v}_{a,1}, \mathbf{v}_{a,2},\ldots,\mathbf{v}_{a,N_t^{RF}}] \in \mathbb{C}^{M \times N_t^{RF}}$ is the analog RF precoder and $\mathbf{V}_d = [\mathbf{v}_{d,1}, \mathbf{v}_{d,2},\ldots,\mathbf{v}_{d,K}] \in \mathbb{C}^{N_t^{RF} \times K}$ is the digital precoder.

Let $\mathbf{s} \in \mathbb{C}^{K \times 1}$, where $E\{\mathbf{s}\mathbf{s}^\dagger\} = \mathbf{I}_K$ is the signal vector transmitted by the BS antenna array and $\mathbf{n}$ is a complex Gaussian noise signal with zero mean and unit variance. The sampled baseband signal received by all users is given by:

$$\mathbf{y} = \mathbf{H}^\dagger \mathbf{V}_a \mathbf{V}_d \mathbf{s} + \mathbf{n} \tag{1}$$

The signal which is received by user k is expressed as follows:

$$\mathbf{y}_k = \tilde{\mathbf{h}}_k^\dagger \mathbf{V}_a \mathbf{V}_d \mathbf{s} + \mathbf{n}_k \tag{2}$$

where $\mathbf{n}_k$ is the additive noise at the kth user. Assuming that the transmitted signals of different users and noise signals are mutually independent, the received signal at the kth user is:

$$\mathbf{y}_k = \tilde{\mathbf{h}}_k^\dagger \mathbf{V}_a \mathbf{V}_{d,k} \mathbf{s}_k + \underbrace{\sum_{\iota=1,\iota \neq k}^{K} \mathbf{h}_\iota^\dagger \mathbf{V}_a \mathbf{V}_{d,\iota} \mathbf{s}_\iota}_{\text{Interference terms}} + \mathbf{n}_k \tag{3}$$

Hence, the downlink Signal-to-Interference-plus-Noise-Ratio (SINR) at the kth user can be represented as:

$$SINR_k = \frac{|\tilde{\mathbf{h}}_k^\dagger \mathbf{V}_a \mathbf{V}_{d,k}|^2}{\sum_{\iota=1,\iota \neq k}^{K} |\tilde{\mathbf{h}}_\iota^\dagger \mathbf{V}_a \mathbf{V}_{d,\iota}|^2 + \sigma_{n,k}^2} \tag{4}$$

In this paper, we assume that both the transmitter and receiver have perfect knowledge of the channel state information (CSI). The achievable average transmission rate of the system can be written as:

$$R_{sum-rate} = \sum_{k=1}^{K} \log_2(1 + SINR_k) \tag{5}$$

2.2. System Model: Wideband Transmission

The transmission model will extended to a hybrid precoding massive MIMO-OFDM system with N subcarriers, in this section. In the OFDM-based hybrid precoding structure, $\mathbf{V}_d[n] = [\mathbf{v}_{d,1}[n], \mathbf{v}_{d,2}[n],\ldots,\mathbf{v}_{d,K}[n]] \in \mathbb{C}^{N_t^{RF} \times K}$ is the digital precoder performing in the frequency domain on a per-subcarrier foundation. The processed signal is then converted to the time domain by applying N-point Inverse Fast Fourier Transforms (IFFTs). $\mathbf{V}_a = [\mathbf{v}_{a,1}, \mathbf{v}_{a,2},\ldots,\mathbf{v}_{a,N_t^{RF}}] \in \mathbb{C}^{M \times N_t^{RF}}$ is the analog RF precoder that is performed in the time domain.

The received signal vector on n^{th} subcarrier of an OFDM symbol after processing is given by:

$$\mathbf{y}[n] = \mathbf{H}^\dagger[n]\mathbf{V}_a \mathbf{V}_d[n]\mathbf{s}[n] + \mathbf{z}[n] \tag{6}$$

where the channel matrix for the nth subcarrier $\mathbf{H}[n] \in \mathbb{C}^{M \times K}$ illustrates physical channel. We suppose that $\mathbf{z}[n]$ is additive white complex Gaussian noise for n^{th} subcarrier, where $\mathbf{z}[n] \sim \mathcal{CN}(0,\sigma^2 \mathbf{I}_K)$.

The signal, which is received by user k is expressed as follows:

$$\mathbf{y}_k[n] = \tilde{\mathbf{h}}_k^\dagger[n]\mathbf{V}_a\mathbf{V}_{d,k}[n]\mathbf{s}_k[n]$$

$$+ \underbrace{\sum_{t=1,t\neq k}^{K}\tilde{\mathbf{h}}_t^\dagger[n]\mathbf{V}_a\mathbf{V}_{d,t}[n]\mathbf{s}_t[n]}_{\text{Interferenceterms}} + \mathbf{z}_k[n] \qquad (7)$$

The channel vector from the kth user is denoted as $\tilde{\mathbf{h}}_k[n] \acute{\mathbf{U}} \mathbf{C}^{M\times 1}$ whose entries are i.i.d. $\mathbf{CN}(0,\delta_k)$ where δ_k represents large scale fading. The downlink channel from BS to the all users in terms of user channel vectors is
$$\mathbf{H}[n] = [\tilde{\mathbf{h}}_1[n],\tilde{\mathbf{h}}_2[n],\ldots,\tilde{\mathbf{h}}_K[n]] = [\mathbf{h}_1[n],\mathbf{h}_2[n],\ldots,\mathbf{h}_M[n]]^T.$$
To model favourable propagation, these channel vectors should be pair-wisely orthogonal. Hence, the downlink SINR at the kth user served on the nth subcarrier can be represented as:

$$SINR_k[n] = \frac{\|\tilde{\mathbf{h}}_k^\dagger[n]\mathbf{V}_a\mathbf{V}_{d,k}[n]\|^2}{\sum_{t=1,t\neq k}^{K}\|\tilde{\mathbf{h}}_t^\dagger[n]\mathbf{V}_a\mathbf{V}_{d,t}[n]\|^2 + \sigma^2} \qquad (8)$$

Then the achievable downlink average transmission rate of the system is:

$$R_{sum-rate}[n] = \sum_{k=1}^{K}\log_2(1 + SINR_k[n]) \qquad (9)$$

2.3. Structure of Clustered Millimeter Wave Channel Model

We consider a clustered mmWave channel model to characterize the sparse scattering features [21]. The narrow mmWave channel matrix can be depicted as:

$$\mathbf{H} = \gamma\sum_{k=1}^{N_{cls}}\sum_{l=1}^{N_{ray}}\alpha_{kl}\mathbf{a}_{t,kl}^*\mathbf{a}_{r,kl} \qquad (10)$$

Where $\gamma = \dfrac{1}{\sqrt{N_{cls}N_{ray}}}$ is a normalization factor.

N_{cls}, denotes the number of clusters and each cluster contains N_{ray} propagation paths and α_{kl} represents the complex gain of the lth ray in the kth cluster, which is assumed to be a zero mean and unit variance complex Gaussian random variable. The azimuth angle of departure $\phi_{a,kl}^t(\phi_{e,kl}^t)$ and azimuth angle of arrival $\phi_{a,kl}^r(\phi_{e,kl}^r)$ are of a truncated Laplacian distribution. The vectors $\mathbf{a}_{t,kl} = \mathbf{a}_t(\phi_{a,kl}^t, \phi_{e,kl}^t)$ and $\mathbf{a}_{r,kl} = \mathbf{a}_r(\phi_{a,kl}^r, \phi_{e,kl}^r)$ are, respectively, the transmit and receive antenna array response vectors of an uniform planar array (UPA) [22]. The array response vector for an UPA with $\sqrt{N}\times\sqrt{N}$ antenna elements is given by:

$$\mathbf{a}(\phi_{a,kl}, \phi_{e,kl}) = \frac{1}{\sqrt{N}}e^{j\frac{2\pi d}{\lambda}(m\cos(\phi_{e,kl}) + w\sin(\phi_{a,kl})\sin(\phi_{e,kl}))} \qquad (11)$$

where d and λ are the antenna spacing and the signal wavelength, and $0 \leq m < \sqrt{N}$, $0 \leq w < \sqrt{N}$ are the antenna indices in the 2D plane.
The frequency domain wideband channel matrix $\mathbf{H}[n]$ for the nth subcarrier can be described as:

$$\mathbf{H}[n] = \gamma\sum_{k=1}^{N_{cls}}\sum_{l=1}^{N_{ray}}\alpha_{kl}\mathbf{a}_{t,kl}^*\mathbf{a}_{r,kl}e^{-j\frac{2\pi}{N}kn} \qquad (12)$$

3. HYBRID PRECODING DESIGN

In this section we discuss hybrid precoding algorithm and we introduce a novel hybrid precoder structure, to achieve a better performance.

3.1. Analog RF Precoder Design

The analog part of the hybrid structure is equipped with analog phase shifters and analog adders. The conventional configuration in analog precoding utilizes a fully-connected structure.

In OFDM-based hybrid massive MIMO, a post-IFFT processing , namely the analog RF precoder, remains constant across all subcarriers [14]. The analog domain is implemented using orthogonal columns selected from a DFT matrix. In contrast the previous works that employed ideal phase shifters in the analog precoding design [14], this paper considers an analog RF precoder architecture based on DFT processing, utilizing an orthogonal precoding codebook.

$$\mathbf{DFT} = \frac{1}{\sqrt{M}}\begin{pmatrix} 1 & 1 & 1 & \ldots & 1 \\ 1 & \omega & \omega^2 & \ldots & \omega^{(N_t^{RF}-1)} \\ 1 & \omega^2 & \omega^4 & \ldots & \omega^{2(N_t^{RF}-1)} \\ \vdots & \vdots & \vdots & \ddots & \vdots \\ 1 & \omega^{(M-1)} & \omega^{2(M-1)} & \ldots & \omega^{(M-1)(N_t^{RF}-1)} \end{pmatrix}$$

(13)

That way, the analog processing can be designed by a Butler matrix integrated as described in [10] that phase shifters are implemented by an integrated circuit.

where $\omega = e^{\frac{-2\pi}{M}}$. The DFT is a special case of quantized candidate precoding matrix. With the orthogonality of DFT codebook that match with the statistical distribution of the optimal precoding weight vectors, makes the DFT-based codebook more efficient in spatially correlated channels [23]. It can reduce the complexity of calculating matrix inverse in hybrid precoding algorithm and most important of all it is more hardware feasible.

3.1.1 Narrowband Transmission

By applying the singular value decomposition (SVD) method on channel matrix [24], the columns of analog precoding matrix $\mathbf{V}_a$ are designed by selecting from the $M \times M$ DFT matrix which represents maximum correlation with the columns of right singular matrix of the channel where the SVD of $\mathbf{H}$ is $\mathbf{H} = \mathbf{U}\mathbf{\Sigma}\mathbf{V}^\dagger$. So it can be written as:

$$V_a(:,\iota) = \max_\iota \langle \mathbf{DFT}(:,\iota), \mathbf{V} \rangle \quad , 1 \le \iota \le N_t^{RF}$$
(14)

where $\mathbf{V}$ is the right singular matrix of the channel.

3.1.2 Wideband Transmission

Similar to the narrowband, the DFT matrix which represents maximum correlation with the columns of the right singular value decomposition (SVD) matrix of the channel where the SVD of $\mathbf{H}[n]$ is

$\mathbf{H}[n] = \mathbf{U}[n]\mathbf{\Sigma}\mathbf{V}^\dagger[n]$, can be given as:

$$V_a(:,\iota) = \max_\iota \langle \mathbf{DFT}(:,\iota), \mathbf{V}[n] \rangle \quad , 1 \le \iota \le N_t^{RF} \quad (15)$$

where $\mathbf{V}[n]$ is the right singular matrix of the channel.

3.2. Proposed Space-Time Coded Hybrid Massive MIMO System Model

This section introduces a STBC hybrid precoding with DFT processing downlink multiuser mmWave MIMO systems. By combining the STBC technique with new hybrid precoding algorithm, the proposed system presents the advantages of both technologies.

3.2.1 Narrowband Transmission

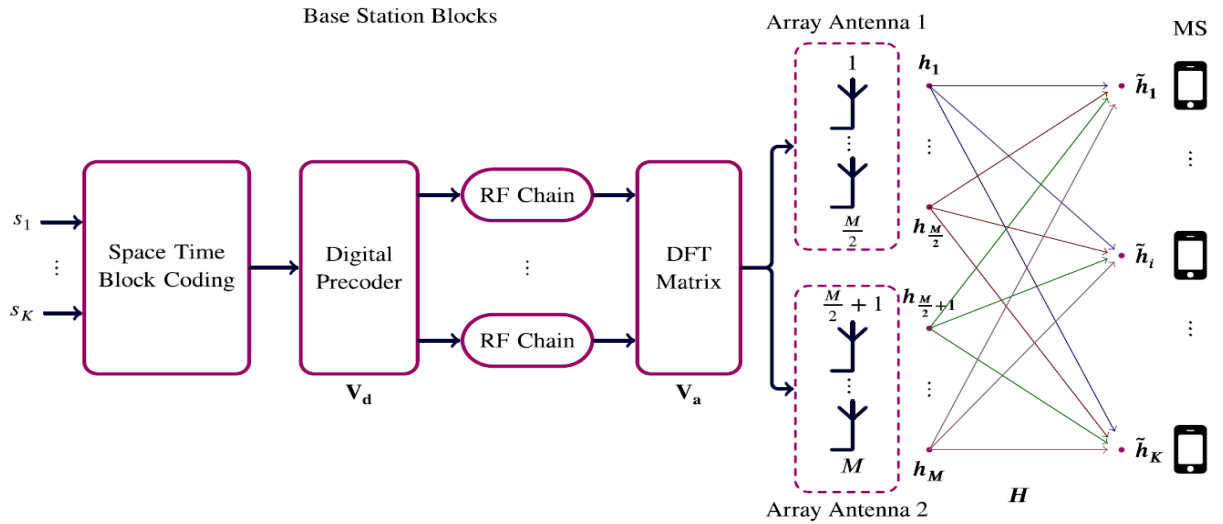The purpose of this subsection is to introduce the proposed system model for the downlink multi-user

Fig. 2. DFT-based Hybrid structure of Space-Time Coded in Narrowband Massive MIMO

STBC hybrid massive MIMO system as shown in Fig. 2. We assume that the BS is equipped with two arrays of transmit antennas that transfer data to K users and there are N_t^{RF} RF chains at the transmitter.

The STBC signal $\mathbf{X} \in \mathbb{C}^{M \times T}$ is transferred from M antennas with a time interval of T to all the users.

The high-dimensional STBC signal is expressed as,

$$\mathbf{X} = \mathbf{VS} \tag{16}$$

where $\mathbf{V} = \mathbf{V}_a\mathbf{V}_d \in C^{M \times K}$ is an equivalent precoding matrix, and $\mathbf{S} \in \mathbb{C}^{K \times T}$ is a low-dimensional STBC.

The received signal follows:

$$\mathbf{Y} = \mathbf{H}^\dagger\mathbf{X} + \mathbf{n} \tag{17}$$

By using the completed $\mathbf{H}_{stbc}$ virtual channel matrix as discussed in [25], we will have:

$$\tilde{\mathbf{Y}} = \mathbf{H}_{stbc}\mathbf{x} + \tilde{\mathbf{n}} \tag{18}$$

Where $\mathbf{x} = \mathbf{Vs} \in C^{M \times 1}$ is the transmitted signal vector in virtual channel and $\tilde{\mathbf{Y}}$ is $T \times K$ the received signal matrix.

$$\begin{pmatrix} \tilde{\mathbf{y}}_1 \\ \tilde{\mathbf{y}}_2^* \\ \tilde{\mathbf{y}}_3^* \\ \vdots \\ \tilde{\mathbf{y}}_{(M^2-M+2)/2}^* \end{pmatrix} = \begin{pmatrix} \mathbf{h}_1 & \mathbf{h}_2 & \mathbf{h}_3 & \dots & \mathbf{h}_{M-1} & \mathbf{h}_M \\ -\mathbf{h}_2^* & \mathbf{h}_1^* & 0 & \dots & 0 & 0 \\ -\mathbf{h}_3^* & 0 & \mathbf{h}_1^* & \dots & 0 & 0 \\ \vdots & \vdots & \vdots & \vdots & \vdots & \vdots \\ 0 & 0 & 0 & \dots & -\mathbf{h}_M^* & \mathbf{h}_{M-1}^* \end{pmatrix} \begin{pmatrix} x_1 \\ x_2 \\ x_3 \\ \vdots \\ x_M \end{pmatrix} + \begin{pmatrix} n_1 \\ n_2^* \\ n_3^* \\ \vdots \\ n_{(M^2-M+2)/2}^* \end{pmatrix}$$
(19)

The estimated received symbol vector $\mathbf{X}$ is obtained as:

$$\tilde{\mathbf{x}} = \mathbf{H}_{stbc}^\dagger \tilde{\mathbf{Y}} = \mathbf{H}_{stbc}^\dagger \mathbf{H}_{stbc}\mathbf{x} + \eta \tag{20}$$

Where the noise terms are obtained $\eta = \mathbf{H}_{stbc}^\dagger \tilde{\mathbf{n}}$, so each estimated symbol can be expressed as:

$$\tilde{x}_\iota = (\| \mathbf{h}_1 \|^2 + \| \mathbf{h}_2 \|^2 + \dots + \| \mathbf{h}_M \|^2)x_\iota + \eta_\iota \tag{21}$$

where $1 \le \iota \le M$.

We can now derive the symbol error rate of quadrature amplitude modulation (QAM) under additive white Gaussian noise, which encode the information in both amplitude and phase. The probability of error P_b for q-QAM can be approximated as [26]:

$$P_b = 2\left(1 - \frac{1}{\sqrt{q}}\right)Q\left(\sqrt{\frac{3}{q-1}SNR}\right) \tag{22}$$

$$SNR = \frac{\left(\sum_{i=1}^{M} \| \mathbf{h}_i \|^2\right)^2}{P_n} \tag{23}$$

where $Q(x) = \frac{1}{2} - \frac{1}{2}erf\left(\frac{x}{2}\right)$ is the Gaussian error function and P_n is noise-power, where $CN(0, \sigma^2)$.

To derive the average BER by using the SNR, we will have:

$$\overline{P_b} = \int_0^\infty P(b \mid \gamma) f_\gamma(\gamma) d\gamma \tag{24}$$

where $P(b \mid \gamma)$ is the bit error probability conditioned on the SNR and $f_\gamma(\gamma)$ is the probability density function (PDF) of the SNR.

To evaluate the probability density function (PDF) of $\gamma = \sum_{i=1}^{M} \| \mathbf{h}_i \|^2$, we know $f_{\gamma_i}(\gamma_i) = e^{-\gamma_i} u(\gamma_i)$ is exponential distribution with $\lambda = 1$, where $\gamma_i = \| \mathbf{h}_i \|^2$. Since γ_i are same and independent random variables, so $f_\gamma(\gamma)$ is convolution of exponential distributions PDFs $f_{\gamma_i}(\gamma_i)$. By applying the Laplace transform we will have:

$$F_\gamma(s) = \prod_{i=1}^{M} F_{\gamma_i}(s) = \prod_{i=1}^{M} \frac{1}{s+1} = \frac{1}{(s+1)^M} \tag{25}$$
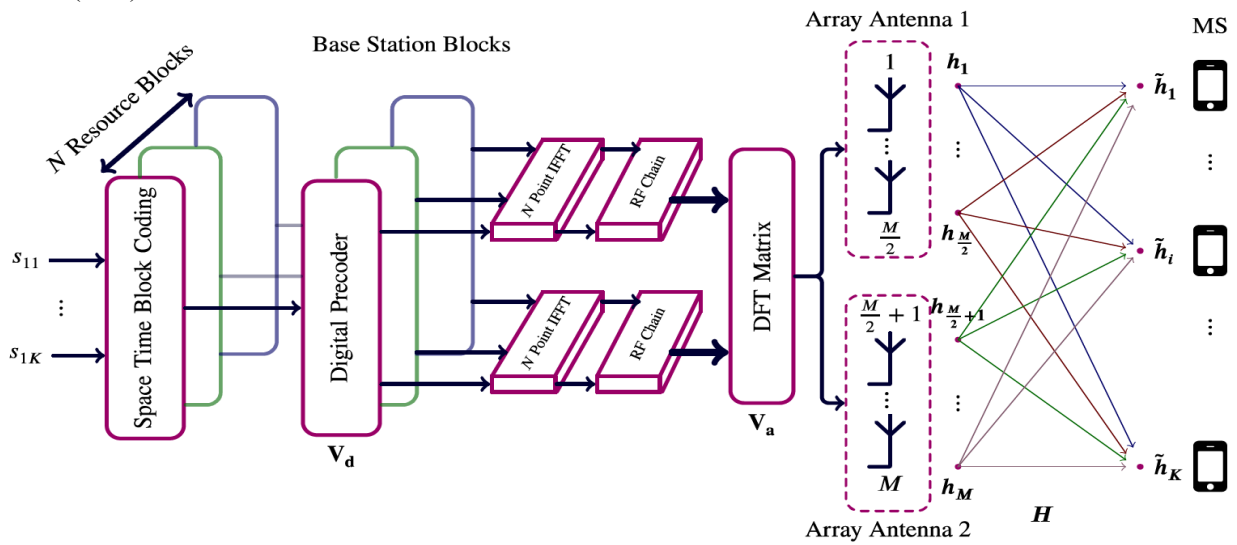

Fig. 3. DFT-based Hybrid Structure of Space-Time Coded in Wideband Massive MIMO

where $F_{\gamma_i}(s)$ is the Laplace transform of $f_{\gamma_i}(\gamma_i)$. So:

$$f_\gamma(\gamma) = \frac{\gamma^{M-1}}{(M-1)!} e^{-\gamma} u(\gamma) \tag{26}$$

$$P(b \mid \gamma) = 2\left(1 - \frac{1}{\sqrt{q}}\right) Q\left(\sqrt{\frac{3}{(q-1)P_n} \gamma}\right) \tag{27}$$

Assuming a large number of antennas, $f_\gamma(\gamma)$ can be approximated based on a Gaussian distribution and can be simplified as follows:

$$f_\gamma(\gamma) \simeq \frac{1}{\sqrt{2\pi\sigma_\gamma^2}} exp\left[-\frac{(\gamma - \bar{\gamma})^2}{2\sigma_\gamma}\right] \tag{28}$$

$$\bar{\gamma} = \left(\sum_{i=1}^{M} \gamma_i\right) = M \overline{\gamma_i} = M \frac{1}{\lambda} = M \tag{29}$$

$$\sigma_\gamma^2 = M \sigma_{\gamma_i}^2 = M \frac{1}{\lambda^2} = M \tag{30}$$

So we have:

$$f_\gamma(\gamma) \simeq \frac{1}{\sqrt{2\pi M}} exp\left[-\frac{(\gamma - M)^2}{2M}\right] \tag{31}$$

Using (27),(31) and $q = 64$ for 64-QAM, the average BER is given by:

$$\overline{P_b} = \int_0^\infty 1.75 Q\left(\sqrt{\frac{0.04}{P_n} \gamma}\right) \frac{1}{\sqrt{2\pi M}} exp\left[-\frac{(\gamma - M)^2}{2M}\right] d\gamma \tag{32}$$

3.2.1 Wideband Transmission

Similar to the previous subsection, we will extend the proposed system model for the downlink multi-user space-time block coded to wideband hybrid massive MIMO system with N subcarriers as shown in Fig.3.

The STBC signal $\mathbf{X}[n] \in \mathbb{C}^{M \times t}$ is transferred from the M antennas with a time interval of t to all the users. The high-dimensional STBC signal is expressed as,

$$\mathbf{X}[n] = \tilde{\mathbf{V}}[n]\mathbf{S}[n] \tag{33}$$

where $\tilde{\mathbf{V}}[n] = \mathbf{V}_a \mathbf{V}_d[n] \in \mathbb{C}^{M \times K}$ is an equivalent precoding matrix, and $\mathbf{S}[n] \in \mathbb{C}^{K \times t}$ is a low-dimensional STBC. The received signal follows:

$$\mathbf{Y}[n] = \mathbf{H}^{\dagger}[n]\mathbf{X}[n] + \mathbf{Z}[n] \qquad (34)$$

where

$$\mathbf{Y}[n] = [\mathbf{y}_1[n], \mathbf{y}_2[n], \ldots, \mathbf{y}_K[n]]^T = [\tilde{\mathbf{y}}_1[n], \tilde{\mathbf{y}}_2[n], \ldots, \tilde{\mathbf{y}}_t[n]] \in C^K$$

is the received signal matrix and $\mathbf{Z}[n]$ is a $K \times t$ noise matrix. We can reduce the complexity of decoupling the space-time transmitted data streams at the receiver side, by applying an equivalent virtual channel matrix. This plan only estimates the M original transmitted signals that received at the mobile station.

By using the completed $\mathbf{H}_{stbc}$ virtual channel matrix as discussed in [25], we will have:

$$\tilde{\mathbf{Y}}[n] = \mathbf{H}_{stbc}[n]\mathbf{x}[n] + \tilde{\mathbf{Z}}[n] \qquad (35)$$

where $\mathbf{x}[n] = \tilde{\mathbf{V}}[n]\mathbf{s}[n] \in C^{M \times 1}$ is the transmitted signal vector in virtual channel and $\tilde{\mathbf{Y}}[n] = [\tilde{\mathbf{y}}_1[n], \tilde{\mathbf{y}}_2^*[n], \ldots, \tilde{\mathbf{y}}_t^*[n]]^T$ is $t \times K$ the received signal matrix.

The estimated transmitted signal vector $\tilde{\mathbf{x}}[n]$ is obtained as:

$$\tilde{\mathbf{x}}[n] = \mathbf{H}_{stbc}^{\dagger}[n]\tilde{\mathbf{Y}}[n] = \mathbf{H}_{stbc}^{\dagger}[n]\mathbf{H}_{stbc}[n]\mathbf{x}[n] + \mathbf{H}_{stbc}^{\dagger}[n]\tilde{\mathbf{Z}}[n] \qquad (36)$$

Each estimated signal vector can be expressed as:

$$\tilde{x}_\iota[n] = (\| \mathbf{h}_1[n] \|^2 + \| \mathbf{h}_2[n] \|^2 + \ldots + \| \mathbf{h}_M[n] \|^2)x_\iota[n] + \mathbf{\eta}_\iota[n] \qquad (37)$$

where $1 \le \iota \le M$ and $\mathbf{\eta}_\iota[n]$ is the noise term.

As explained in the narrowband transmission to calculate the average BER by using the SNR over N subcarriers, we act as follows:

$$SNR[n] = \frac{\left(\sum_{i=1}^{M} \| \mathbf{h}_i[n] \|^2\right)^2}{P_n[n]} \qquad (38)$$

$$\gamma[n] = \sum_{i=1}^{M} \| \mathbf{h}_i[n] \|^2 \qquad (39)$$

$$\overline{P}_b = \int_0^{\infty} P(b \mid \overline{\gamma[n]}) f_\gamma(\gamma[n]) d\gamma \qquad (40)$$

where $P(b \mid \gamma[n])$ is the bit error probability conditioned on the SNR and $f_\gamma(\gamma[n])$ is the probability density function (PDF) of the SNR.

To evaluate the probability density function (PDF) of $\gamma[n] = \sum_{i=1}^{M} \| \mathbf{h}_i[n] \|^2$, we know $f_{\gamma_i}(\gamma_i[n]) = e^{-\gamma_i[n]}u(\gamma_i[n])$ is exponential distribution with $\lambda = 1$, where $\gamma_i = \| \mathbf{h}_i \|^2$. Since γ_i are same and independent random variables, so $f_\gamma(\gamma[n])$ is convolution of exponential distributions PDFs $f_{\gamma_i}(\gamma_i)$. By applying the Laplace transform we will have:

$$F_\gamma(s) = \prod_{i=1}^{M} F_{\gamma_i}(s) = \prod_{i=1}^{M} \frac{1}{s+1} = \frac{1}{(s+1)^M} \qquad (41)$$

where $F_{\gamma_i}(s)$ is the Laplace transform of $f_{\gamma_i}(\gamma_i[n])$. So:

$$f_\gamma(\gamma[n]) = \frac{\gamma^{M-1}[n]}{(M-1)!} e^{-\gamma[n]} u(\gamma[n]) \qquad (42)$$

$$P(b \mid \gamma[n]) = 2\left(1 - \frac{1}{\sqrt{q}}\right) Q\left(\sqrt{\frac{3}{(q-1)P_n[n]}} \gamma[n]\right) \qquad (43)$$

Assuming a large number of antennas, $f_\gamma(\gamma[n])$ can be approximated based on a Gaussian distribution and can be simplified as follows:

$$f_\gamma(\gamma[n]) \simeq \frac{1}{\sqrt{2\pi\sigma_\gamma^2[n]}} exp\left[-\frac{(\gamma[n] - \overline{\gamma}[n])^2}{2\sigma_\gamma[n]}\right] \qquad (44)$$

$$\overline{\gamma}[n] = \overline{\left(\sum_{i=1}^{M} \gamma_i[n]\right)} = M \gamma_i[n] = M \frac{N}{\lambda} = NM \qquad (45)$$

$$\sigma_\gamma^2[n] = M \sigma_{\gamma_i[n]}^2 = M \frac{N}{\lambda^2} = NM \qquad (46)$$

So we have:

$$f_\gamma(\gamma[n]) \simeq \frac{1}{\sqrt{2\pi NM}} exp\left[-\frac{(\gamma[n] - NM)^2}{2NM}\right] \qquad (47)$$

Using (43),(47) and $q = 64$, the average BER is given by:

$$\overline{P}_b = \int_0^{\infty} 1.75 Q\left(\sqrt{\frac{0.04}{P_n}} \gamma[n]\right) \frac{1}{\sqrt{2\pi NM}} exp\left[-\frac{(\gamma[n] - NM)^2}{2NM}\right] d\gamma \qquad (48)$$

As mentioned before, we consider a SVD hybrid massive MIMO transmission.

So to estimate the low-dimensional STBC signal vector $\tilde{\mathbf{s}}[n]$, the virtual channel matrix can be decomposed by using SVD method as follows:

$$\mathbf{U}_{stbc}[n] = (\mathbf{U}_{stbc,1}[n] \mathbf{U}_{stbc,2}[n]) \qquad (49)$$

$$\mathbf{\Sigma}_{stbc} = \begin{pmatrix} \Sigma_{stbc,1} & 0 \\ 0 & \Sigma_{stbc,2} \end{pmatrix} \qquad (50)$$

$$\mathbf{V}_{stbc}^{\dagger}[n] = \begin{pmatrix} \mathbf{V}_{stbc,1}^{\dagger}[n] \\ \mathbf{V}_{stbc,2}^{\dagger}[n] \end{pmatrix} \qquad (51)$$

$$\mathbf{H}_{stbc}[n] = \mathbf{U}_{stbc}[n]\mathbf{\Sigma}_{stbc}\mathbf{V}_{stbc}^{\dagger}[n] = \mathbf{U}_{stbc,1}[n]\mathbf{\Sigma}_{stbc,1}\mathbf{V}_{stbc,1}^{\dagger}[n] + \mathbf{U}_{stbc,2}[n]\mathbf{\Sigma}_{stbc,2}\mathbf{V}_{stbc,2}^{\dagger}[n] \qquad (52)$$

where $\mathbf{U}_{\mathbf{stbc,1}}[n] \in \mathbb{C}^{t \times K}$ and $\mathbf{V}_{\mathbf{stbc,1}} \in \mathbb{C}^{M \times K}$ are semi-unitary matrices containing the first K columns of unitary matrices $\mathbf{U}_{\mathbf{stbc}}[n]$ and $\mathbf{V}_{\mathbf{stbc}}[n]$, respectively. $\mathbf{\Sigma}_{\mathbf{stbc,1}}$ is a $K \times K$ non-negative diagonal matrix. We consider Maximum Eigen Beamforming (MEB) which is the optimal scheme in terms of the SNR. Thus, by using this kind of decomposition, (35) is written as:

$$\tilde{\mathbf{Y}}[n] = \mathbf{U}_{\mathbf{stbc}}[n]\mathbf{\Sigma}_{\mathbf{stbc}}\mathbf{V}_{\mathbf{stbc}}^{\dagger}[n]\mathbf{x}[n] + \tilde{\mathbf{Z}}[n]$$
$$= \mathbf{U}_{\mathbf{stbc}}[n]\mathbf{\Sigma}_{\mathbf{stbc}}\mathbf{V}_{\mathbf{stbc}}^{\dagger}[n]\tilde{\mathbf{V}}[n]\mathbf{s}[n] + \tilde{\mathbf{Z}}[n] \quad (53)$$

Multiply by $\mathbf{U}_{\mathbf{stbc}}^{\dagger}[n]$ from left:

$$\tilde{\mathbf{s}}[n] = \mathbf{U}_{\mathbf{stbc}}^{\dagger}[n]\tilde{\mathbf{Y}}[n] = \mathbf{\Sigma}_{\mathbf{stbc}}\mathbf{V}_{\mathbf{stbc}}^{\dagger}[n]\mathbf{V}[n]\mathbf{s}[n]$$
$$+\mathbf{U}_{\mathbf{stbc}}^{\dagger}[n]\tilde{\mathbf{Z}}[n] \quad (54)$$

Let the equivalent precoding matrix $\tilde{\mathbf{V}}[n] = \mathbf{V}_{\mathbf{stbc,1}}[n]$, with fully-digital SVD-based precoding, we will have:

$$\tilde{\mathbf{s}}[n] = (\mathbf{\Sigma}_{\mathbf{stbc,1}}\mathbf{V}_{\mathbf{stbc,1}}^{\dagger}[n])\mathbf{V}_{\mathbf{stbc,1}}[n]\mathbf{s}[n]$$
$$+(\mathbf{\Sigma}_{\mathbf{stbc,2}}\mathbf{V}_{\mathbf{stbc,2}}^{\dagger}[n])\mathbf{V}_{\mathbf{stbc,1}}[n]\mathbf{s}[n] + \mathbf{U}_{\mathbf{stbc}}^{\dagger}[n]\tilde{\mathbf{Z}}[n]$$
$$= \mathbf{\Sigma}_{\mathbf{stbc,1}}\mathbf{s}[n] + \mathbf{U}_{\mathbf{stbc}}^{\dagger}[n]\tilde{\mathbf{Z}}[n] \quad (55)$$

The estimation procedure can be developed by the hybrid precoder optimization problem as is introduced in the next section.

3.3. Proposed Hybrid Precoding Algorithm

An effective hybrid algorithm in wideband will be proposed to optimize the digital and analog precoders. The proposed hybrid precoding algorithm represented in Algorithm 1, uses analog precoding based on the DFT processing that reduces hardware complexity compared to the fully-connected structure.

We provide an algorithmic hybrid precoding solution inspired from the AltMin algorithm which is updated by the LSA. The corresponding problem is equivalent to minimize the Euclidean distance between the optimal fully-digital precoder and the hybrid precoders (maximizes the spectral efficiency expression).

The hybrid precoder optimization problem can be stated as follows:

$$\{\mathbf{V}_{a,opt}, \mathbf{V}_{d,opt}[n]\} = \arg\min_{\mathbf{V}_a, \mathbf{V}_d[n]} \sum_{n=0}^{N-1} \| \mathbf{V}_{opt}[n] - \mathbf{V}_a\mathbf{V}_d[n] \| \quad (56)$$

$$s.t. \quad \mathbf{V}_a(:,\iota) = \max_{\iota}\langle \mathbf{DFT}(:,\iota), \mathbf{V}_{opt}[n]\rangle, 1 \leq \iota \leq N_t^{RF}$$

$$\sum_{n=1}^{N} \| \mathbf{V}_a\mathbf{V}_d[n] \|^2 = NK$$

where $\mathbf{V}_{opt}[n]$ stands for the optimal fully digital precoder and it is comprised of the first K columns of $\mathbf{V}_{\mathbf{stbc}}[n]$ which is a unitary matrix derived from the channel SVD in the proposed system. $\mathbf{V}_a, \mathbf{V}_d$ respectively, are the analog and digital precoders to be optimized.

Algorithm 1. Proposed Algorithm.

DFT-Based Alternating Minimization with the Least Squares Amendment

---

Require $\mathbf{V}_{opt}[n]$

1. Construct an initial point for $\mathbf{V}_a$ according to DFT-Based Matrix (13).
2. Repeat
3. **For** $n = 1,\ldots,N$ do
4. Fix $\mathbf{V}_a$ solving $\mathbf{V}_d$ using the SVD:
5. $\mathbf{U}[n]\mathbf{\Sigma}\mathbf{V}^{\dagger}[n] = \mathbf{V}_{opt}^{\dagger}[n]\mathbf{V}_a$
6. $\mathbf{V}_d[n] = \mathbf{V}[n]\mathbf{U}^{\dagger}[n]$
7. **For** $n = 1,\ldots,N$ do
8. **For** $\iota = 1,\ldots,N_t^{RF}$ do
9. $\mathbf{V}_a(:,\iota) = \max_{\iota}\langle \mathbf{DFT}(:,\iota), \mathbf{V}_{opt}[n]\mathbf{V}_d^{\dagger}[n]\rangle$
10. End For
11. End For
12. End For
13. **Until** a stopping criterion triggers.
14. Update by Least Squares Amendment (LSA):
15. **For** $n = 1,\ldots,N$ do
16. $\mathbf{V}_d[n] = (\mathbf{V}_a^{\dagger}\mathbf{V}_a)^{-1}\mathbf{V}_a^{\dagger}\mathbf{V}_{opt}[n]$
17. End For
18. For the digital precoder at the transmit end, normalize $\mathbf{V}_d[n] = \dfrac{\sqrt{K}}{\| \mathbf{V}_a\mathbf{V}_d[n] \|}\mathbf{V}_d[n]$
19. Return $\mathbf{V}_a, \mathbf{V}_d[n]$

Algorithm 1 presents a step-by-step summary of the proposed algorithm. The algorithm simplifies the problem by optimizing one of $\mathbf{V}_a, \mathbf{V}_d$ while fixing the other. The iterations continue until $\| \mathbf{V}_{opt}[n] - \mathbf{V}_a\mathbf{V}_d[n] \|^2 \leq \acute{\mathbf{U}}$ drops below the specified convergence threshold. In the first step, by providing an initial version for $\mathbf{V}_a$ using a low-complexity codebook-based algorithm, we select the columns of $\mathbf{V}_a$ from the DFT codebook whose columns contain orthogonal beamforming vectors. After the initialization of $\mathbf{V}_a$, the digital precoder $\mathbf{V}_d$ can be determined by using the least square solution. In the next alternating step, $\mathbf{V}_d$ is fixed and update $\mathbf{V}_a$ by deciding:

$$\mathbf{V}_a(:,\iota) = \max_{\iota}\langle \mathbf{DFT}(:,\iota), \mathbf{V}_{opt}[n]\mathbf{V}_d^{\dagger}[n]\rangle \quad (57)$$

The final digital baseband precoding matrix improves with LSA. The proposed narrowband algorithm can be provided similar to wideband algorithm.

4. COMPUTATIONAL COMPLEXITY

The computational complexity analysis of hybrid precoding methods, particularly in the context of mmWave massive MIMO systems, reveals significant insights into their efficiency and

performance. Here's a summary based on the provided search results:

* The DFT codebook-based hybrid precoding method leverages an orthogonal codebook for beam selection, which allows for efficient analog precoding [27].

* The AltMin method operates by iteratively minimizing a cost function with respect to different sets of variables (e.g., analog and digital precoders). The overall complexity can be expressed as: O(I·f(n)) where I is the number of iterations to convergence and f(n) is the complexity of each minimization step [14].

In conclusion, while the AltMin method provides a flexible framework for optimizing hybrid precoding in massive MIMO systems, its computational complexity can be significant depending on the number of iterations required for convergence and the specific minimization steps involved. The proposed method employs an iterative algorithm that simplifies matrix operations, leading to faster convergence and lower overall computation time compared to conventional approaches. For instance, our iterative approach significantly reduces the need for matrix inversion, which is often a computational bottleneck in massive MIMO systems.

Compared to DFT-based approaches AltMin can offer competitive performance but may incur higher computational costs in certain scenarios.

Table 1. Computational Complexity

| Algorithm	Median operation
Fully-digital	$\bigcirc(M^3)$
DFT-based Hybrid Precoding	$\bigcirc(MK^2 + K^2)$
AltMin	$\bigcirc(I f(n))$
Proposed Algorithm	$\bigcirc(I(MK^2 + K^2))$

5. SIMULATION RESULTS

The performance analysis of the proposed structure by simulation results is presented in this section. In the clustered channel model, we assume $N_{cls} = 3$ clusters and $N_{ray} = 10$ rays, and the simulation results are averaged over 1000 channel realizations.

In our study, we assume that the CSI is obtained through a standard estimation process, which typically involves pilot signaling and feedback mechanisms. With perfect CSI, the BER is minimized since the transmitter can
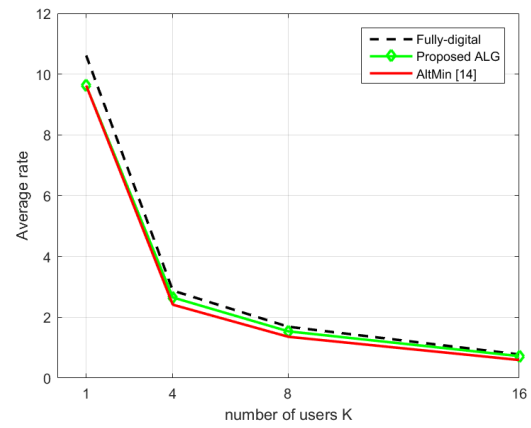
a) Narrowband
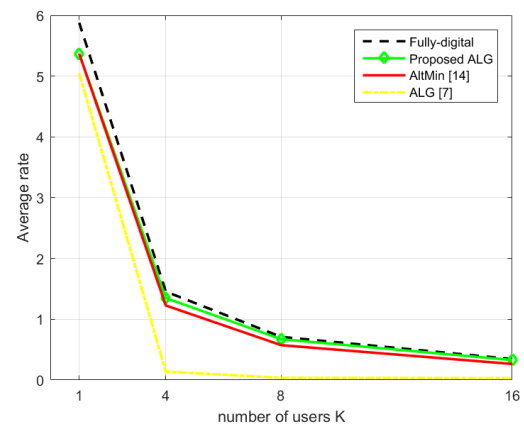
b) Wideband

Fig. 4. Average rate vs. numbers of users for SNR= 5dB

precisely adjust its transmission parameters (such as power and modulation schemes) to match the channel conditions. As a result, the system achieves its theoretical limits for BER. We demonstrate the average rate performance and BER performance by using the proposed structure for downlink multiuser transmission scenario when $M = 64$, $K = 16$ and we assume that the number of subcarriers is $N = 128$. The number of RF chains is the same as the number of users K.

5.1. Spectral Efficiency Evaluation

Firstly, we illustrate the spectral efficiency achieved by different algorithms when the number of RF chains is equal to that of the data streams, i.e., $N_t^{RF} = N_s = K$.

When $N_t^{RF} = N_s = K$, there exists a closely solution to the design of the fully-connected hybrid precoding, which leads to the same spectral efficiency provided by the optimal fully-digital precoding.

We show in Fig. 4 the average transmission rate per user as a function of K for SNR=5dB for the proposed algorithm and other structures (fully-digital, Proposed Algorithm without STBC , AltMin [14] and ALG [7]). The average rate decreases with the number of users. The gap between the fully-digital and hybrid precoding cases decrease with K.

Fig. 5 depicts the average transmission rate of the proposed scheme versus the input SNR in narrowband and wideband, respectively.
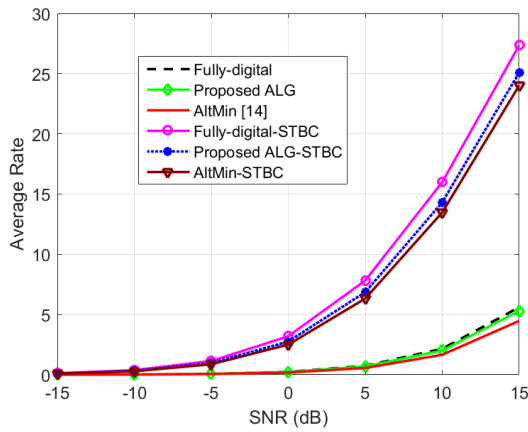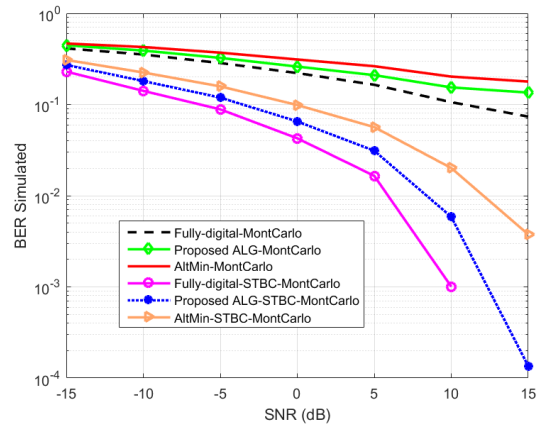
a)   Narrowband
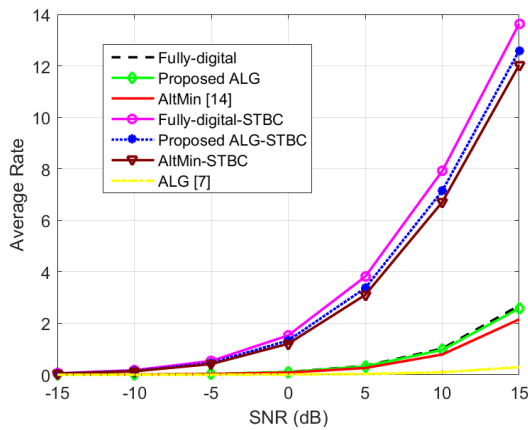
b)   Wideband

Fig. 5. Average transmission rate versus SNR with K = 16
For comparison, we illustrate the average transmission rate versus SNR for different structures in conventional versions (fully-digital, Proposed Algorithm without STBC, AltMin [14] and ALG [7]) and STBC-based designs (fully-digital-STBC, Proposed Algorithm-STBC and AltMin-STBC).
As expected the performance gains of fully-digital architecture always outperforms the hybrid
architectures, regardless of ideal phase shifters and DFT precessing.

5.2.   Received SNR and BER Evaluation

The Monte Carlo method is the most popular method used to estimate the BER of a communication system. This approach involves simulating the transmission of K data symbols through a model of the digital communication system under study. During the simulation, we count the number of errors that occur at the receiver to derive the BER. The simulation incorporates pseudo-random data and various noise sources, alongside the signal processing models available within the system. By processing a substantial number of symbols through this simulation framework, we can accurately estimate the performance metrics. Additionally, we will conduct experimental validations to complement our simulation results, ensuring a comprehensive evaluation of the proposed method's effectiveness.
In Fig. 6, we present the Monte Carlo BER performance of the STBC-based hybrid architecture with DFT
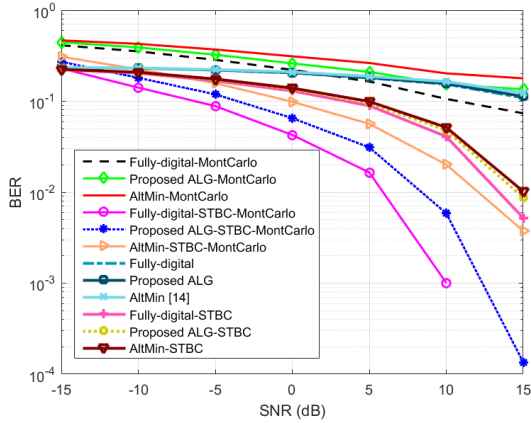

a)   Narrowband
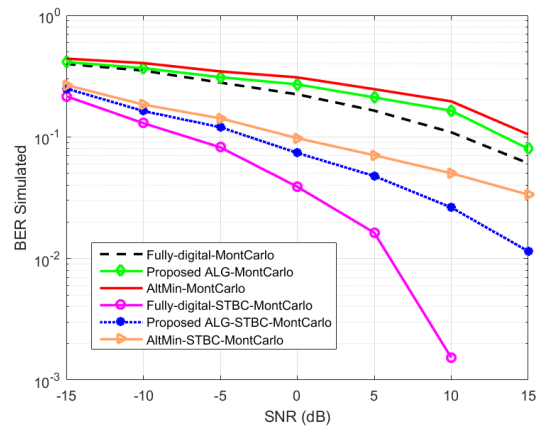
b)   Wideband

Fig. 6. Monte Carlo BER performance (withM = 64, K = 16)

plotted against the SNR. The results indicate that the BER performance and average transmission rate of the STBC-based hybrid architecture with DFT processing outperform those of existing hybrid architectures utilizing ideal phase shifters.
Furthermore, the diversity gains are evident from the increased slope observed at high SNR levels, highlighting the effectiveness of the proposed architecture in enhancing communication reliability under challenging conditions. In this section, we utilize Monte Carlo simulations as a numerical method to investigate and validate our analytical expression for the BER of 64-QAM modulation. As illustrated in Fig. 7, we compare the numerical analysis of the BER performance for 64-QAM modulation with the corresponding BER values derived from our analytical formula (32). The results demonstrate a strong correlation between the analytically obtained BER and the values obtained from the Monte Carlo simulations, confirming the accuracy of our analytical model. This agreement suggests that our analytical expression reliably predicts the performance of 64-QAM modulation under various conditions.
Furthermore, the Monte Carlo simulations allow us to explore a range of scenarios, including different Signal-to-Noise Ratios (SNRs) and noise conditions, thereby providing a comprehensive understanding of the system's

performance. Overall, these findings reinforce

a)   Narrowband
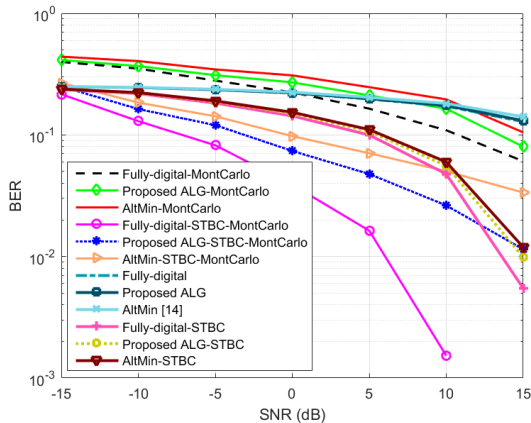
b)   Wideband

Fig. 7. BER performance comparison (Numerical Simulations V.s. Analytical Formula) (with M = 64, K = 16)

the validity of our analytical approach while highlighting the robustness of 64-QAM modulation in practical applications.

6.   CONCLUSIONS

This paper introduces a space-time coded hybrid precoding method with DFT processing for downlink multiuser mmWave MIMO systems.

We propose an effective algorithm for hybrid precoding structures that operates efficiently in both narrowband and wideband scenarios. Simulation results are presented to highlight several valuable design insights derived from our approach. In the proposed architecture, the analog domain employs DFT processing, which contributes to low-cost implementation and high efficiency. The hybrid precoder utilizing DFT processing achieves performance levels comparable to those of fully digital precoders, demonstrating its effectiveness in practical applications. Moreover, our design harnesses the advantages of STBCs, providing transmit diversity in both narrowband and OFDM-based systems. This integration results in superior performance compared to conventional structures, particularly in terms of average transmission rate and error rate. By combining space-time coding techniques with a novel hybrid precoding algorithm, our system leverages the strengths of both technologies. The results clearly indicate that the proposed design not only achieves a comparable transmission rate but also realizes near-

optimal performance gains similar to those obtained with unconstrained fully digital precoding.

7.   AUTHOR DECLARATIONS

- Availability of data and materials:
  Not applicable
- Competing interests:
  The authors have no conflicts of interest to declare that are relevant to the content of this article.
- Funding:
  No funding was received to assist with the preparation of this manuscript.

8.   REFERENCE

[1] Dilli R, "Performance analysis of multi user massive MIMO hybrid beamforming systems at millimeter wave frequency bands", Wireless Networks, pp. 1–15, 2021.

[2] Lee YY, Wang CH, Huang YH, "A hybrid RF/baseband precoding processor based on parallel-index-selection matrix-inversion-bypass simultaneous orthogonal matching pursuit for millimeter wave MIMO systems", IEEE Transactions on Signal Processing,63(2):305–317, 2015.

[3] Abose, Tadele A and Olwal, Thomas O and Daniel, Abel D and Hassen, Murad R "Performance Comparison of Hybrid Switch, Phase Shifter and Lens Network over Hybrid Beamforming in Millimeter Wave Massive MIMO", Iranian Journal of Electrical & Electronic Engineering, vol. 20, no. 3, 2024.

[4] Dilli R, "Hybrid beamforming in 5G NR networks using multi user massive MIMO at FR2 frequency bands", Wireless Personal Communications, no. 127(4), pp. 3677–3709, 2022.

[5] Zang G, Hu L, Yang F, Ding L, Liu H, "Partially-Connected Hybrid Beamforming for Multi-User Massive MIMO Systems", IEEE Access, no. 8, pp. 215287–215298, 2020.

[6] Qiao X, Zhang Y, Zhou M, Yang L, "Alternating optimization based hybrid precoding strategies for millimeter wave MIMO systems", IEEE Access, no. 8, pp. 113078–113089, 2020.

[7] Moradi, Amirreza, and Nasim Jafari Farsani, "A Dynamic Hybrid Precoding Structure for mmWave Massive MIMO Systems", International Journal of Information and Communication Technology Research vol. 16, no. 1, pp. 1-10, 2024.

[8] Yu X, Zhang J, Letaief KB, "Doubling phase shifters for efficient hybrid precoder design in millimeter-wave communication systems" Journal of Communications and Information Networks, no. 4(2), pp. 51–67, 2019.

[9] Molisch AF, Zhang X, Kung SY, Zhang J. "DFT-based hybrid antenna selection schemes for spatially correlated MIMO channels", 14th IEEE Proceedings on Personal, Indoor and Mobile Radio Communications. vol. 2, pp. 1119–1123, 2003.

[10] Garcia-Rodriguez A, Venkateswaran V, Rulikowski P, Masouros C, "Hybrid analog–digital precoding revisited under realistic RF modeling", IEEE Wireless Communications Letters, no. 5(5), pp. 528–531, 2016.

[11] Tan W, Matthaiou M, Jin S, Li X, "Spectral efficiency of DFT-based processing hybrid architectures in massive MIMO", IEEE Wireless Communications Letters, no. 6(5), pp. 586–589, 2017.

[12] Liu Y, Zhang Q, He X, Lei X, Zhang Y,Qiu T, "Spectral-efficient hybrid precodingfor multi-antenna multi-user mmWave massive MIMO systems with low complexity", EURASIP Journal on Wireless Communications and Networking, no.1, pp. 1–19, 2022.

[13] Wong SS, Teng CF, Wu AY, "Two-Step Codebook-Assisted Alternating Minimization (CA-AltMin) for Low-Complexity Hybrid Beamforming Design", IEEE Communications Letters, 2021.

[14] Yu X, Shen JC, Zhang J, Letaief KB, "Alternating minimization algorithms for hybrid precoding in millimeter wave MIMO systems", IEEE Journal of Selected Topics in Signal Processing, no. 10(3), pp. 485–500, 2016.

[15] Soleimani M, Elliott RC, Krzymie´n WA, Melzer J, Mousavi P, "Hybrid beamforming for mmWave massive MIMO systems employing DFT-assisted user clustering", IEEE Transactions on Vehicular Technology, no. 69(10), pp. 11646–11658, 2020.

[16] Alamouti SM. "A simple transmit diversity technique for wireless communications", IEEE Journal on selected areas in communications, no. 16(8), pp. 1451–1458, 1998.

[17] Ice JJ, Abdolee R, Vakilian V, "Space-Time Coded Massive MIMO for Next Generation Wireless Systems", International Conference on Wireless Networks (ICWN), July 2017.

[18] Iqbal S, Hamamreh JM, "Modified MU-STBC with Round Transmission for Improving the Date Rate and Reliability of Future 6G and Beyond Wireless Networks", RS Open Journal on Innovative Communication Technologies, no. 3(8) , 2023.

[19] Lau, Christopher M, "Performance of MIMO Systems Using Space Time Block Codes (STBC)", Open Journal of Applied Sciences vol. 11, no. 3, pp.273, 2021.

[20] Meng X, Xia XG, Gao X, "Omnidirectional STBC design in massive MIMO systems", IEEE Global Communications Conference (GLOBECOM), pp. 1–6 2015.

[21] H. Jiang, M. Mukherjee, J. Zhou et al., "Channel modeling and characteristics for 6G wireless communications", IEEE Network, no. 35(1), pp. 296–303, 2021.

[22] Akdeniz MR, Liu Y, Samimi MK, Sun S, Rangan S, Rappaport TS, et al, "Millimeterwave channel modeling and cellular capacity evaluation", IEEE journal on selected areas in communications, no. 32(6), pp. 1164–1179, 2014.

[23] Yang D, Yang LL, Hanzo L, "DFT-based beamforming weight-vector codebook design for spatially correlated channels in the unitary precoding aided multiuser downlink", IEEE International Conference on Communications (ICC), pp. 1–5, 2010.

[24] F.R. Castillo-Soria, C.A. Gutierrez, A. García-Barrientos et al., "EQSM-based multiuser MIMO downlink transmission for correlated fading channels", EURASIP J. Wirel. Commun. Netw, 2020.

[25] Nieh JY, Tummala M, Vincent P, "A Systematic Approach to the Design of Space-Time Block Coded MIMO Systems", Fortieth Asilomar Conference on Signals, Systems and Computers, pp. 1296–1299, 2006.

[26] Goldsmith, Andrea, "Wireless communications", Cambridge university press, 2005.

[27] Huang, Yu, et al. "DFT codebook-based hybrid precoding for multiuser mmWave massive MIMO systems." EURASIP Journal on Advances in Signal Processing, pp. 1-13, 2020.